

Lyotropic liquid crystalline cellulose derivatives in blends and molecular composites

J. M. G. Cowie^{* a}, Valeria Arrighi^a, Juliet Cameron^a, Dean Robson^b

^aDept. of Chemistry, Heriot-Watt University, Edinburgh, EH14 4AS, Scotland

^bThe Scottish College of Textiles, Netherdale, Galashiels, TD1 3HF, Scotland

SUMMARY: Cellulose tricarbanilate (CTC)/ methylacrylate (MA) solutions were prepared and the methylacrylate polymerised to produce a series of molecular composites. The solutions were studied using polarised microscopy. The mechanical properties and morphology of the composites were investigated using dynamic mechanical thermal analysis (DMTA) and scanning electron microscopy (SEM). Although the SEM micrographs for composites with <45 wt % CTC revealed an apparent one-phase system, DMTA measurements indicated the existence of a double T_g . The 45 wt % CTC composites however showed a broad relaxation process with a third T_g corresponding to the glass transition of the CTC itself. This result which is indicative of phase separation, is consistent with the SEM micrographs showing distinctive layered structures within the film.

Introduction

Molecular composites have been defined by Helminiak et al.^{1,2)} as miscible blends of rigid-rod and flexible-coil polymers where the rigid reinforcing component is dispersed at the molecular level in the flexible coil matrix. These materials present several advantages over conventional fibre reinforced composites due to the absence of the fibre-matrix interface. However, as proposed originally by Flory et al.^{3,4)}, the major drawback to preparing true molecular composites lies in the inherent immiscibility between rigid rod and flexible coils. Many rigid or semi-rigid main chain molecules form liquid crystalline phases either in solution (*lyotropic*) or in a given temperature range (*thermotropic*) and many studies have been devoted to the use of liquid crystalline polymers (LCPs) as the reinforcing component in polymer blends⁵⁾. The molecular orientation in the LCP tends to enhance the mechanical strength and improve the thermal and mechanical resistance of the blends but usually a multiphase rather than a single phase system is obtained. This phase separation can be overcome if the orientation of the rigid-rod polymer can be “locked in” by *in situ*

polymerisation of a polymerizable solvent *i.e.* a monomer⁶⁻¹¹).

Cellulose is a poly(1,4- β -D-glucosan) with a persistence length generally around 10 nm that characterises it as a semi-rigid polymer¹²). While the naturally occurring materials are difficult to dissolve, an extensive range of derivatives, which are soluble in organic solvents, can be prepared by substitution of the hydroxyl groups which are soluble in organic solvents. Many cellulose derivatives form both lyotropic and thermotropic liquid crystalline phases¹³), particularly cholesteric mesophases because of the chiral nature of the cellulose chains. As cellulose is a naturally occurring, renewable, biodegradable polymer, composites prepared from cellulose derivative/synthetic monomer systems, with good mechanical properties, are of enormous potential interest.

In this study, we focus on the properties of composites prepared from isotropic and anisotropic solutions of cellulose tricarbanilate (CTC) and methyl acrylate (MA) by *in situ* photopolymerization of the MA monomer. Although the preparation, morphology and optical properties of similar composites have been already reported, studies of the mechanical behaviour of these materials are limited¹⁴). In addition, the relationship between mechanical properties and structure/morphology is still poorly understood and we therefore attempt to provide a link between dynamic mechanical thermal analysis (DMTA) data and scanning electron microscopy (SEM) analysis.

Materials

Cellulose tricarbanilate was produced using the following heterogeneous method. Dry cellulose powder (30 mmoles) (Aldrich Chemical Co. ~20 microns) was soaked in distilled pyridine (250 cm³) for 2 hours under a nitrogen atmosphere. Phenylisocyanate (270 mmoles) was then added dropwise and the mixture was refluxed at 115°C for 5 hours. A clear brown viscous solution was produced which was concentrated and precipitated into methanol. Purification of the CTC by four re-precipitations from acetone solution into methanol and a final precipitation from ethyl acetate into methanol produced a white flaky powder. The powder was dried *in vacuo* at 60°C overnight to produce CTC with a degree of substitution of 2.96 from elemental analysis.

Sample preparation

A range of solutions, from 0 to 45 wt % CTC, were prepared in methylacrylate (MA). All solutions had 0.01 % photoinitiator added (Daro Cur 1173 - Ciba Speciality Chemicals) and were left for 2 weeks to homogenise. The viscous solutions were spread quickly into a custom built cell and polymerised under a UV lamp ($3400 \mu\text{W}/\text{cm}^2$ at 46 cm in the 360 nm region) for 10 minutes. The films (approximately 0.75 mm thick) were left for a further 30 min before drying overnight *in vacuo* at 60°C. CTC samples for DMTA measurements were prepared by first impregnating a fiber glass support with a CTC solution in acetone and then evaporating the solvent.

Measurements

The CTC/MA solutions were analysed using an Olympus BH-2 Polarised Optical Microscope (POM) fitted with a Linkam 'PR 600' hot stage. Clearing temperatures were determined by observing the disappearance of the birefringent textures while heating the samples under the POM.

Dynamic mechanical thermal analysis (DMTA) was carried out on a Mark 1 Polymer Lab DMTA. The samples were run on a dual cantilever flexure mode operating at $\times 1$ strain, oscillating frequency of 1 Hz and a heating rate of 5°C min^{-1} . Both the loss (E'') and the storage (E') moduli were recorded in the temperature range from 150 to 495 K. An exponentially modified Gaussian function was used to fit the DMTA $\tan \delta (= E''/E')$ curves.

Topographical analysis of the freeze fractured surfaces was carried out using a Hitachi S-530 scanning electron microscope (SEM). The SEM samples were gold sputter coated to approximately 20 nm and imaged using an accelerating voltage of 10 kV.

Results and discussion

CTC dissolves readily in MA and forms optically clear, anisotropic solutions above the critical concentration of 33 wt % CTC. Sanded nematic birefringent textures are observed for all the solutions in the CTC/MA series. A cholesteric liquid crystalline phase is only produced on shearing of the solutions containing 45 wt % CTC whereas at lower CTC content no cholesteric

texture is observed after shearing. Figure 1 shows the typical grandjean textures exhibited by the induced cholesteric phase of the 45 wt % CTC/MA solution.

The thermal stability of the lyotropic solutions is shown in Figure 2 where the clearing temperatures have been plotted versus CTC concentration. As the CTC content increases, a rise in the clearing temperature is observed, indicating an increasing thermal stability of the system. At 45 wt % CTC, the onset concentration for the cholesteric phase, the clearing temperature decreases possibly due to the transition from the nematic mesophase to the chiral phase.

The CTC/poly(methyl acrylate) (PMA) composites were prepared by polymerising the MA matrix around the CTC thus 'freezing in' the lyotropic liquid crystalline order. The translucent films exhibit increased rigidity compared to the original PMA sample with the stiffness escalating to produce a brittle composite at 45 wt % CTC.



Fig.1: Polarised micrograph of 45 wt % CTC in methylacrylate, obtained after shearing

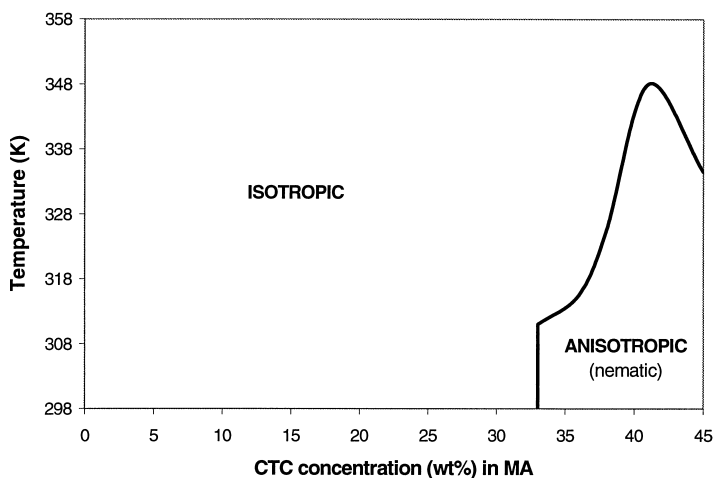


Fig.2: Schematic phase diagram of CTC/methylacrylate solutions

The DMTA measurements illustrate the effect of the CTC as a stiffening agent. For all samples investigated, the storage modulus shows a continuous drop at the glass transition (T_g) which shifts towards higher temperature as the CTC content increases. This shift is accompanied by a broadening of the T_g region. The high temperature plateau of the modulus occurs at higher values with increasing CTC concentration.

The damping behaviour, expressed as $\tan\delta$, provides more detailed information on the physical and mechanical properties of the polymer composites.

Figure 3 shows the $\tan\delta$ plots for the CTC/PMA composite series from 15 wt % CTC to 45 wt % CTC. As discussed for the storage modulus, T_g values shift to higher temperatures with increasing CTC content and the glass transition region broadens. In addition, the shape and character of the $\tan\delta$ curves varies with the CTC concentration. While the $\tan\delta$ curve of PMA (not shown in Figure 3) exhibits a sharp peak indicative of a homogeneous system, for CTC contents ranging between 15 wt % and 30 wt %, the $\tan\delta$ peaks are broad and a secondary relaxation process is observed as a shoulder above the original T_g . Above 30 wt %, the $\tan\delta$ peaks are sharp and the secondary relaxation process is observed as a shoulder above the original T_g .

CTC the secondary shoulder is no longer discernible and a much broader, less intense, asymmetrical curve is produced. The 45 wt % CTC sample still exhibits a broad asymmetric $\tan \delta$ peak, but an additional relaxation is observed at 490 K. This corresponds to the glass transition of the pure CTC sample.

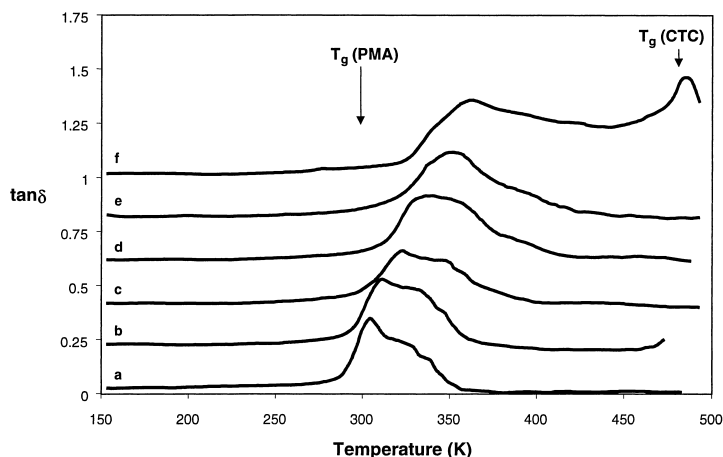


Fig 3: $\tan \delta$ vs temperature of CTC. PMA composites: (a) 15 wt % CTC, (b) 20 wt % CTC, (c) 30 wt % CTC, (d) 35 wt % CTC, (e) 40 wt % CTC, (f) 45 wt % CTC. The data have been displaced vertically by a $\tan \delta$ of 0.2 for clarification

Further analysis of the $\tan \delta$ curves was carried out by curve fitting using an exponentially modified Gaussian (EMG) function. Figure 4 gives an example of a $\tan \delta$ peak and corresponding data fit. Two exponentially modified Gaussian functions were used to separate the two relaxation processes and the maxima, T_{g1} and T_{g2} , were recorded. It is found that, although both T_{g1} and T_{g2} values rise with increasing CTC content, there is an approximately steady temperature difference between T_{g1} and T_{g2} which corresponds to 10 degrees. A detailed analysis of the DMTA data will be reported in a separate publication.

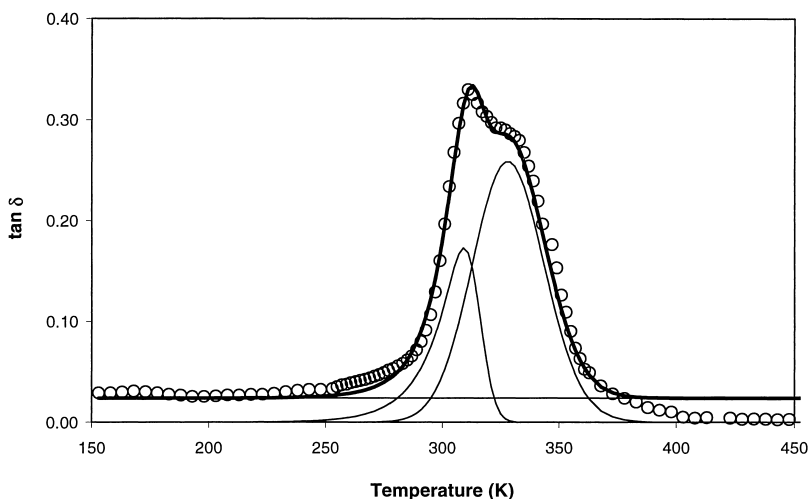


Fig 4: Tan δ data for 20wt% CTC/PMA with EMG curve fitting:
 O experimental data, — Curve fitted data

It has long been recognised that the mechanical properties of a polymer system greatly depend on its morphology and structure¹⁵. As expected for a miscible blend, the broad relaxation process occurs at a temperature which is intermediate between the T_g s of the pure components but the existence of a shoulder on the tan δ plots for 15 wt % to 30 wt % samples suggests that the composites are not homogeneous. It is possible that a dual morphology system could result from the biphasic, *i.e* isotropic/anisotropic, nature of the polymerised films.

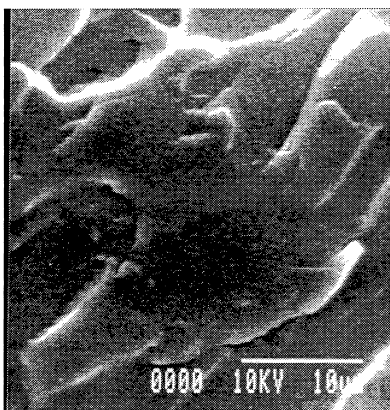
Alternatively, the double T_g could result from the varying degrees of mobility of the PMA chains within the composites. Tsagaropoulos and Eisenberg¹⁶ have observed similar double T_g results for several polymers containing fine silica particles. The first glass transition was identified with the normal polymer T_g , whereas the second one was attributed to polymer chains with reduced mobility. The existence of two T_g s is therefore a result of heterogeneously distributed regions of different mobility.

Similarly, the DMTA data for the CTC/PMA composites indicate that these materials are characterised by regions with different chain mobilities and are therefore not homogeneous. However, the difference between the two T_g s is small compared to that observed for the

filler/polymer systems (60 to 100 °C). At low CTC concentration (15 wt % CTC) the $\tan \delta$ peak is mainly due to the PMA chains. We suggest that the rigid CTC chains impart some restriction on the mobility of neighbouring PMA chains. This is indicated by the higher glass transition of the 15 wt % sample compared to pure PMA. In addition, those PMA segments which are closer to the CTC chains are affected more and this results in the appearance of a second relaxation process at higher temperature. As the concentration of CTC increases from 15 to 30 wt %, the PMA motion becomes increasingly restricted: both T_{g1} and T_{g2} values increase.

Above 30 wt % CTC, it is no longer possible to distinguish two $\tan \delta$ peaks and only a broad asymmetric relaxation shifted towards higher temperature is observed. The breadth of the relaxation process makes it difficult to comment on the homogeneous/heterogeneous nature of the composite.

a)



b)

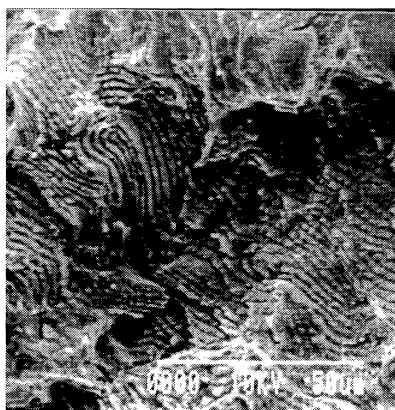


Fig 5: SEM micrograph of 20 wt % CTC/PMA composite (a); and SEM micrograph of 45 wt % CTC/PMA composite (b)

The morphology of the 15 to 30 wt % samples was investigated by SEM analysis. Figure 5(a) shows a micrograph typical of the freeze fracture surfaces from the 15 to 30 wt % CTC composition region. Although these samples appeared to be slightly opaque, no phase

separation can be observed in the micrographs. This result does not exclude that a certain degree of microphase separation may occur in these composites and we are currently investigating this possibility using light scattering and small angle X-ray scattering.

The SEM micrographs of the 35 and 40 wt % CTC composites indicate that these samples have similar topographical textures and as shown in Figure 5(b) gross phase separation is observed for the sample with 45 wt % CTC.

This result for the 45 wt % composite confirms the DMTA data (Figure 3) where a high temperature $\tan\delta$ peak corresponding to the T_g of pure CTC was observed. The phase separation process produces periodic lamellar like structures that develop throughout the film fracture surface. Some areas of the layering are reminiscent of the cholesteric fingerprint textures which are usually observed in cholesteric LCs using optical microscopy. As the CTC/MA solutions formed nematic textures, the SEM results suggest that the polymerisation process induces formation of the cholesteric ordering of the CTC in the PMA matrix.

Conclusion

CTC dissolves readily in MA and forms nematic liquid crystalline solutions above 33 wt % CTC concentration. The polymerisation of the MA around the CTC produces composites in which the PMA matrix entraps the liquid crystalline character of the CTC solutions. The morphology and structure of the composites are investigated by DMTA and SEM analysis. The mechanical properties of CTC/PMA composites are directly influenced by their internal structure and it is argued that the nature of the original solutions is intrinsic to the composites mechanical response. The DMTA data indicate that microphase separation occurs in the CTC/PMA composites at concentrations as low as 15 wt % CTC, as shown by the presence of two overlapping $\tan \delta$ peaks. Although the composites are heterogeneous up to 30 wt % CTC, gross phase separation can be detected only for samples containing 45 wt % CTC by both DMTA and SEM analysis.

It may be suggested that the polymerisation induces cholesteric liquid crystalline order at lower CTC concentrations than observed for the original solutions.

Acknowledgement

J.D. Cameron gratefully appreciates funding from EPSRC.

References

- ¹⁾ T.E. Helminiak, F.E. Arnold and C.L. Benner, *ACS. Polymer Prep.* **16**, 659 (1975)
- ²⁾ T.E. Helminiak, *Div. Org. Coat. Plast. Chem. Prep.* **40**, 475 (1979)
- ³⁾ A. Abe and P.J. Flory, *Macromolecules* **11**, 1122 (1978)
- ⁴⁾ P.J. Flory, *Macromolecules* **11**, 1138 (1978)
- ⁵⁾ A.I. Isayev, T. Kyn and S.Z.D. Cheng "Liquid-crystalline polymer Systems - Technological Advances" *ACS Symp. Series* 632 (1996)
- ⁶⁾ T. Tsutsui and R.Tanaka, *J. Polym. Sci., Polym. Lett. Ed.* **18**, 17 (1980)
- ⁷⁾ T. Tsutsui and R.Tanaka, *Polymer* **22**, 117 (1981)
- ⁸⁾ Y. Nishio, T. Yamana and S. Takahashi, *J. Polym. Sci., Phys. Ed.* **23**, 1043 (1985)
- ⁹⁾ J.J. Kozakiewicz, *Macromolecules* **19**, 1262 (1986)
- ¹⁰⁾ J.J. Kozakiewicz, *J. Appl. Polym. Sci.* **34**, 1109 (1987)
- ¹¹⁾ S.H. Jiang and Y. Huang, *J. Appl. Polym. Sci.* **49**, 125 (1993)
- ¹²⁾ D.G. Gray and R.R. Harkness, in "Liquid Crystalline and Mesomorphic Polymers", V.P. Shibaev and L. Lam, Springer-Verlag 1993 , p. 295
- ¹³⁾ D.G. Gray, *Applied Polym. Symp.* **37**, 179 (1983)
- ¹⁴⁾ S.H. Jiang, Y. Huang and J.R. Shen, *J. Appl. Polym. Sci.* **57**, 493 (1995)
- ¹⁵⁾ S.H. Jaing and Y.Huang, *J. Appl. Polym. Sci.* **50**, 607 (1993)
- ¹⁶⁾ G. Tsagaropoulos and A. Eisenberg, *Macromolecules* **28**, 6067 (1995)